

Advancements in Translation Accuracy for Stereo Visual-Inertial Initialization

1st Han Song
Computer Science
University of Southern California
California, USA
hsong427@usc.edu

2nd Zhongche Qu*
Computer Science
Columbia University
New York, USA
zq2172@columbia.edu

3rd Zhi Zhang
Computer Science
New York University
New York, USA
zz2310@nyu.edu

4th Zihan Ye
Technopreneurship and Innovation
Nanyang Technological University
Singapore, Singapore
yezi0004@e.ntu.edu.sg

5th Cong Liu
Computer Science
Harbin Institute of Technology
Shenzhen, China
liucong@stu.hit.edu.cn

Abstract—As the current initialization method in the state-of-the-art Stereo Visual-Inertial SLAM framework, ORB-SLAM3 has limitations. Its success depends on the performance of the pure stereo SLAM system and is based on the underlying assumption that pure visual SLAM can accurately estimate the camera trajectory, which is essential for inertial parameter estimation. Meanwhile, the further improved initialization method for ORB-SLAM3, known as Stereo-NEC, is time-consuming due to applying keypoint tracking to estimate gyroscope bias with normal epipolar constraints. To address the limitations of previous methods, this paper proposes a method aimed at enhancing translation accuracy during the initialization stage. The fundamental concept of our method is to improve the translation estimate with a 3 Degree-of-Freedom (DoF) Bundle Adjustment (BA), independently, while the rotation estimate is fixed, instead of using ORB-SLAM3’s 6-DoF BA. Additionally, the rotation estimate will be updated by considering IMU measurements and gyroscope bias, unlike ORB-SLAM3’s rotation, which is directly obtained from stereo visual odometry and may yield inferior results when operating in challenging scenarios. We also conduct extensive evaluations on the public benchmark, the EuRoC dataset, demonstrating that our method excels in accuracy.

Index Terms—component, formatting, style, styling, insert

I. INTRODUCTION

The combination of cameras and Inertial Measurement Units (IMUs) is highly effective for environmental sensing. Cameras capture a rich, detailed representation of the environment, while IMUs measure acceleration and angular velocity, providing robustness against fast motion and environments with little texture, as well as resilience to variations such as changes in lighting or motion blur. Together, these sensors complement each other perfectly. By harnessing both cameras and IMUs, Visual-Inertial SLAM (VI-SLAM) systems can accurately determine the metric six degrees-of-freedom (DOF) state [1]–[3]. Meanwhile, VI-SLAM systems are widely used in various fields and applications where accurate localization and mapping are crucial. These include autonomous vehicles [4]–[7], autonomous robots [8]–[11], augmented reality

(AR) and virtual reality (VR) [12]–[14], manipulation [15] and underwater applications [16] such as marine archaeology, computer vision [17]. Additionally, VI-SLAM systems are essential for effective path planning [11], [18], 3D reconstruction [19]–[25] and plane reconstruction [26], [27].

However, while monocular VI-SLAM systems, which utilize a single camera and IMU, are cost-effective, they encounter several limitations, such as up-to-scale maps and a restricted field of view (FOV). Consequently, roboticists are increasingly adopting stereo VI-SLAM systems that use a stereo camera setup. This configuration offers enhanced capabilities, enabling the reconstruction of 3D geometry even without requiring camera motion.

There are many factors that impact the performance of stereo VI-SLAM systems in terms of accuracy. Initialization is a critical issue that affects the accuracy and usability of VI-SLAM. Moreover, initialization is the first step in running VI-SLAM because it is necessary to recover gravity, initial velocity, acceleration, and gyroscope biases, all of which are essential for the effective use of stereo VI-SLAM. A good initialization is crucial for stereo VI-SLAM, requiring not only the accurate recovery of scale, gravity, initial velocity, acceleration, and gyroscope biases to enable the use of VI-SLAM, but also providing a solid initial value that serves as a good seed for the stereo VI-SLAM system.

Similar to the initialization methods used in monocular VI-SLAM systems, as described in various studies [12], [28]–[36], stereo VI-SLAM initialization can be divided into two categories: joint approaches [31], [37] and disjoint approaches [38]–[42]. The key difference between joint and disjoint methods is whether an additional Structure-from-Motion (SfM) problem is required, with inertial parameters subsequently derived based on trajectory from pure visual SLAM. In this paper, we focus on the disjoint method because it typically yields more accurate results than the joint method. The joint method often overlooks the gyroscope bias in its

closed-form solution, which can lead to limited accuracy and is computationally expensive [36].

As an initialization method for stereo VI-SLAM, VINS-Fusion [40], building on VINS-Mono [12], adopts a slightly different approach by jointly estimating velocity, gravity vector, and scale via visual-inertial bundle adjustment, rather than addressing them separately. In a similar vein, ORB-SLAM3 [41] integrates the inertial-only optimization-based approach [35] into their stereo VI-SLAM system. Meanwhile, Stereo-NEC [42] enhances ORB-SLAM3 by improving both rotation and trajectory estimation. This is achieved by utilizing stereo normal epipolar constraints to determine the initial gyroscope bias and employing it to initiate a Maximum A Posteriori (MAP) problem for further refinement of inertial parameters. Additionally, it separates the estimation of rotation using IMU integration, leveraging precise rotation estimates to improve translation estimation through 3-DoF bundle adjustment.

While ORB-SLAM3 generally assumes accurate camera trajectory estimation in scenarios with sufficient baseline between consecutive frames [42], its initialization also suffer in challenging conditions, such as during intense or pure rotation, leading to decreased accuracy and robustness. Additionally, while Stereo-NEC improves upon the methods used in ORB-SLAM3, it suffers from significant runtime delays due to the feature matching required when estimating gyroscope bias through eigenvalue-based optimization.

This need highlights the requirement for methods that can deliver improved performance in term of accuracy while maintaining a comparable run-time speed. In response, we propose a method called ETA, which focuses on enhancing translation accuracy during the initialization stage. The core principle of our method is to refine the translation estimate using a 3 Degree-of-Freedom (DoF) Bundle Adjustment (BA), conducted independently, while keeping the rotation estimate fixed, as opposed to employing ORB-SLAM3's 6-DoF BA. Furthermore, unlike ORB-SLAM3, where the rotation is derived directly from stereo visual odometry and might perform suboptimally in tough scenarios, our approach updates the rotation estimate by taking into account IMU measurements and gyroscope bias. Additionally, our method aims to achieve performance comparable to Stereo-NEC while maintaining a runtime similar to that of ORB-SLAM3.

II. PRELIMINARIES

A. Inertial Residual

The inertial residual, $r\mathcal{L}_{k-1,k}$, at time k is defined as:

$$\begin{aligned} r\mathcal{L}_{k-1,k} &= [r\Delta\mathbf{R}_{k-1,k}, r\Delta\mathbf{V}_{k-1,k}, r\Delta\mathbf{t}_{k-1,k}]^\top \\ r\Delta\mathbf{R}_{k-1,k} &= \log(\Delta\mathbf{R}_{k-1,k}^\top \mathbf{R}_{k-1}^\top \mathbf{R}_k) \\ r\Delta\mathbf{V}_{k-1,k} &= \mathbf{R}_{k-1}^\top (\mathbf{V}_k - \mathbf{V}_{k-1} - \mathbf{g}\Delta t_{k-1,k} - \Delta\mathbf{V}_{k-1,k}) \\ r\Delta\mathbf{t}_{k-1,k} &= \mathbf{R}_{k-1}^\top (\mathbf{t}_k - \mathbf{t}_{k-1} - \mathbf{V}_{k-1}\Delta t_{k-1,k} - \frac{1}{2}\mathbf{g}\Delta t_{k-1,k}^2) - \Delta\mathbf{t}_{k-1,k} \end{aligned}$$

where \mathbf{R}_{k-1} and \mathbf{R}_k denote the rotations relative to the world frame, and $\Delta\mathbf{R}_{k-1,k}$, $\Delta\mathbf{V}_{k-1,k}$, and $\Delta\mathbf{t}_{k-1,k}$ are the IMU pre-integration of rotation, velocity, and position measurements

receptively and \mathbf{g} is a gravity vector represented in world frame. $\Delta\mathbf{t}_{k-1,k}$ represents an interval between two consecutive frames.

B. Visual Residual

The visual residual, $r\mathcal{L}_{reproj}$, at time k is defined as:

$$\begin{aligned} r\mathcal{L}_{reproj} &= \mathbf{x}^i - \pi(\cdot)(\mathbf{R}_{c_k,w}\mathbf{X}^i + \mathbf{t}_{c_k,w}) \\ \pi_m\left(\begin{bmatrix} X \\ Y \\ Z \end{bmatrix}\right) &= \begin{bmatrix} f_x \frac{X}{Z} + c_x \\ f_y \frac{Y}{Z} + c_y \end{bmatrix}, \pi_s\left(\begin{bmatrix} X \\ Y \\ Z \end{bmatrix}\right) = \begin{bmatrix} f_x \frac{X}{Z} + c_x \\ f_y \frac{Y}{Z} + c_y \\ f_x \frac{X-b}{Z} + c_x \end{bmatrix}, \end{aligned}$$

where \mathbf{X}^i represents a 3D point in the world frame, derived through stereo matching given a known baseline or triangulation, while \mathbf{x}^i denotes the corresponding 2D feature. The functions $\pi(\cdot)$ refer to the reprojection processes, with π_m for monocular and π_s for rectified stereo reprojection. $[X, Y, Z]^\top$ represents a 3D point coordinate, f_x and f_y are focal length, c_x and c_y are the principal point and b is the baseline of a stereo camera.

C. Visual-Inertial Residual

Considering the combination of visual and inertial residuals, we can formulate the objective function for the entire Visual-Inertial SLAM (VI-SLAM) system as follows:

$$\begin{aligned} \mathbf{e} &= r\mathcal{L}_{k-1,k} + r\mathcal{L}_{reproj} \\ \min_{\mathcal{X}} &= \sum ||r\mathcal{L}_{k-1,k}||_{\Sigma_{k-1,k}}^2 + \sum ||r\mathcal{L}_{reproj}||_{\Sigma_{k-1,k}}^2 \end{aligned}$$

where $\Sigma_{k-1,k}$ represents the corresponding covariance matrix for the inertial residual, and $\Sigma_{k-1,k}$ for the visual residual. Additionally, \mathcal{X} denotes the state that the VI-SLAM system needs to estimate.

III. PROPOSED APPROACH

Our method is inspired by Stereo-NEC [42], which demonstrate that translation accuracy with 3-DoF bundle adjustment, when combined with precise rotation, is more accurate than a 6-DoF bundle adjustment. Building on Stereo-NEC, we separately estimate rotation using IMU integration, leveraging precise rotation estimates to enhance translation estimation through 3-DoF bundle adjustment. The underlying concept of our method combines the ORB-SLAM3 [41] method with the 3-DoF steps of Stereo-NEC to enhance initialization performance. We start by formulating a MAP problem for estimating inertial parameters and then proceed to update rotation estimation and then we use it to enhance translation estimation in term of accuracy.

Our method, as shown in 1, involves four steps aimed at deriving precise initial values for keyframes' poses and velocities, gravity direction, and IMU biases:

- **Step 1. Pure Stereo Visual SLAM:** We recover the initial camera poses from stereo visual-only SLAM.
- **Step 2. Inertial-only Optimizer:** We estimate keyframes' velocities, gravity direction, gyroscope bias and acceleration bias by solving an inertial-only MAP estimation problem.

- **Step 3. Rotation-Translation-Decoupled Strategy:** We release the camera rotation estimate by integrating gyroscope measurements with the gyroscope bias removed, and optimize the camera translation using 3-DoF BA from Stereo-NEC.
- **Step 4. Joint Visual-Inertial Bundle Adjustment:** We utilize the solution derived from the previous steps as the initial estimate and construct a joint visual-inertial Maximum A Posteriori (MAP) problem to obtain optimal estimates for all inertial parameters, camera poses, and 3D landmark estimates.

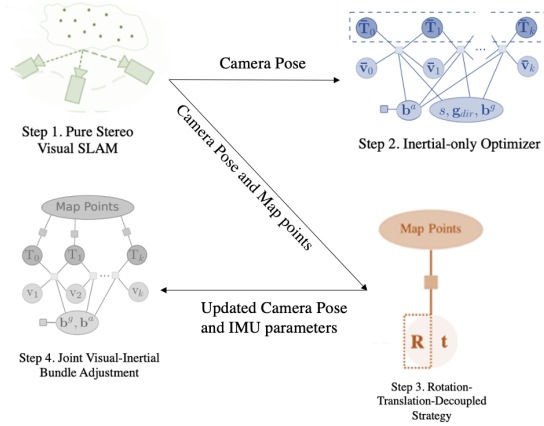


Fig. 1: A diagram of the proposed pipeline. Initially, it runs pure stereo SLAM, followed by using an inertial-only optimizer to estimate inertial parameters. Next, it employs an efficient 3-DoF BA to enhance the translation estimates. Finally, it optimizes the entire set of visual and inertial parameters jointly through joint Visual-Inertial BA.

A. Pure Stereo Visual SLAM

Compared to monocular SLAM systems, Stereo SLAM systems provide a wider field of view (FOV) and offer the advantage of a known baseline. This allows Stereo SLAM systems to directly recover 3D landmarks with scale, even in static or pure rotation scenarios.

In this step, we run stereo SLAM with Bundle Adjustment using both Monocular and Stereo Constraints to estimate camera poses. The optimization employs the Levenberg-Marquardt method implemented in g2o, a non-linear optimization framework designed specifically for SLAM purposes.

Specifically, the Stereo SLAM system estimates camera poses, denoted as $[\mathbf{R}_{c_k, w}, \mathbf{t}_{c_k, w}]$, by minimizing the reprojection error between matched 3D points in the world frame and their corresponding keypoints, whether they are monocular or stereo keypoints, as shown is Equation 1:

$$\{\mathbf{R}_{c_k, w}, \mathbf{t}_{c_k, w}\} = \arg \min_{\mathbf{R}_{c_k, w}, \mathbf{t}_{c_k, w}} \sum_{i \in \mathcal{M}} \rho(\|\mathbf{x}^i - \pi(\cdot)(\mathbf{R}_{c_k, w} \mathbf{X}^i + \mathbf{t}_{c_k, w})\|_{\Sigma}^2) \quad (1)$$

where \mathbf{X}^i represents a 3D point in the world frame, derived through stereo matching given a known baseline, while \mathbf{x}^i denotes the corresponding 2D feature. The robust Huber

cost function is denoted by ρ . The functions $\pi(\cdot)$ refer to the reprojection processes, with π_m for monocular and π_s for rectified stereo reprojection. Additionally, Σ signifies the covariance associated with the scale level of the keypoints within the pyramid, as detailed in [13].

B. Inertial-only Optimizer

In this step, our goal is to derive estimates for keyframes' velocities, the direction of gravity, and IMU biases through Maximum A Posteriori (MAP), which incorporates an empirical prior residual. Practically, this is achieved by using ORB-SLAM3's Inertial-only MAP Estimation method. This method relies on keyframes within a sliding window and the inertial measurements recorded between these keyframes.

C. Rotation-Translation-Decoupled Strategy

Drawing inspiration from Stereo-NEC, we also apply a Rotation-Translation-Decoupled Strategy to enhance the accuracy of translation estimates. Stereo-NEC demonstrates that, after obtaining an optimal gyroscope bias from Step 2, updating each rotation estimate within the sliding window through IMU rotation integration, and optimizing each translation with only 3-DoF Bundle Adjustment (BA), can achieve more accurate results than the traditional 6-DoF BA. This traditional approach simultaneously considers rotation and translation estimates during the optimization phase.

Therefore, the first part of this step involves obtaining the rotation by using IMU integration, with the gyroscope bias removed following the Inertial-only optimizer step. Subsequently, we apply 3-DoF Bundle Adjustment (BA) to the translation, as shown in Equation 2:

$$\begin{aligned} \mathbf{R}_{w, c_k} &= \mathbf{R}_{w, b_k} \mathbf{R}_{b, c} \\ \mathbf{t}_{c_k, w}^* &= \arg \min_{\mathbf{t}_{c_k, w}} \sum_{i \in \mathcal{M}} \rho(\|\mathbf{x}^i - \pi(\cdot)(\mathbf{R}_{c_k, w} \mathbf{X}^i + \mathbf{t}_{c_k, w})\|_{\Sigma}^2) \end{aligned} \quad (2)$$

The rotation \mathbf{R}_{w, b_k} is obtained from IMU integration with the gyroscope bias removed, and $\mathbf{R}_{b, c}$ represents the IMU-Camera extrinsic matrix derived from calibration and it is worth noting that \mathbf{R}_{w, c_k} is fixed during optimization.

D. Joint Visual-Inertial Bundle Adjustment

Our final step involves applying Joint Visual-Inertial Bundle Adjustment, considering both inertial and visual residuals once we have a good estimation of inertial and visual parameters. This step aims to further refine the estimates of inertial parameters, camera poses, and 3D landmark positions through a joint visual-inertial optimization.

IV. EVALUATION

A. Experiment Results

To assess accuracy across different sequences, we conducted an exhaustive initialization test. In this test, we initiated an initialization every 2.5 seconds for each sequence, resulting in the evaluation of 464 distinct initialization segments. Table I presents a comparison of rotation errors between our results and those obtained by ORB-SLAM3, while Table II displays

the absolute trajectory errors. Both tables include data with and without integration with visual-inertial bundle adjustment. Our method outperforms ORB-SLAM3 in several machine hall environments, specifically in the V1_01 and V2_03 machine halls in terms of rotation error, and in the V2_02 machine hall in terms of absolute trajectory error. Overall, our method produces results that are comparable to those of ORB-SLAM3. Specifically, our results outperform those of ORB-SLAM3 on the Vicon Room 2-3(V2_03_difficult) dataset in both Absolute Trajectory Error and Rotation Error. This achievement is particularly noteworthy given the challenges presented by the Vicon Room 2-3(V2_03_difficult) dataset, which includes motion blur and illumination changes. These factors pose significant difficulties for the state estimator.

MHall & VRoom	Rotation Error			
	Without VI-BA		With VI-BA	
	ORB-SLAM3	Ours	ORB-SLAM3	Ours
MH_01_easy	0.083	0.084	0.020	0.019
MH_02_easy	0.093	0.093	0.016	0.016
MH_03_medium	0.344	0.335	0.036	0.037
MH_04_difficult	0.165	0.171	0.032	0.035
MH_05_difficult	0.153	0.169	0.028	0.030
V1_01_easy	0.188	0.193	0.115	0.112
V1_02_medium	0.448	0.405	0.065	0.064
V1_03_difficult	0.892	0.924	0.095	0.095
V2_01_easy	0.177	0.190	0.042	0.040
V2_02_medium	0.320	0.328	0.076	0.070
V2_03_difficult	0.987	0.910	0.214	0.224
Avg	0.350	0.345	0.067	0.067

TABLE I: Comparison of rotation error between ours results and ORB-SLAM3 results in without VI-BA and with VI-BA

MHall VRoom	Absolute Trajectory Error			
	Without VI-BA		With VI-BA	
	ORB-SLAM3	Ours	ORB-SLAM3	Ours
MH_01_easy	0.007	0.007	0.004	0.004
MH_02_easy	0.006	0.006	0.004	0.004
MH_03_medium	0.034	0.034	0.012	0.012
MH_04_difficult	0.027	0.028	0.014	0.014
MH_05_difficult	0.023	0.026	0.011	0.012
V1_01_easy	0.008	0.008	0.006	0.005
V1_02_medium	0.022	0.020	0.007	0.006
V1_03_difficult	0.052	0.054	0.009	0.008
V2_01_easy	0.006	0.006	0.003	0.003
V2_02_medium	0.019	0.021	0.007	0.006
V2_03_difficult	0.056	0.055	0.016	0.016
Avg	0.023	0.024	0.008	0.008

TABLE II: Comparison of Absolute Trajectory Error error between ours results and ORB-SLAM3 results in without VI-BA and with VI-BA

B. Environment setup and implementation

The EuRoC dataset offers highly accurate rotational and transactional data for 11 Micro Air Vehicle(MAV) sequences, covering a range of flight conditions. This dataset includes synchronized visual inertial sensor units equipped with global

shutter cameras and a MEMS inertial Measurement Unit(IMU) that provides angular rage and acceleration data. Additionally, it provides camera intrinsic parameters and camera-IMU extrinsic parameters. All experiments were conducted on an Intel i7-9700k desktop computer with 64 GB of RAM. To ensure an equitable comparison between the initialization methods of ORB-SLAM3 and Stero-NEC, our method was integrated into ORB-SLAM3. In all our evaluations, the absolute trajectory error(ATE) was measured in meters without involving scale alignment.

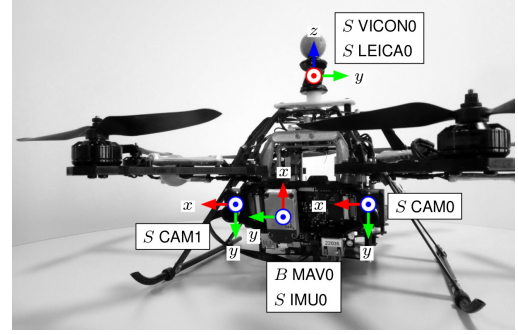


Fig. 2: An Asctec Firefly hex-rotor aerial drone was used, equipped with a visual-inertial sensor unit comprising a camera and an IMU.

V. CONCLUSIONS

In conclusion, this study addresses the limitations of the current initialization methods in the state-of-the-art Stereo Visual-Inertial SLAM framework, specifically ORB-SLAM3 and its improved version, Stereo-NEC. ORB-SLAM3's reliance on the pure stereo SLAM system for accurate camera trajectory estimation and inertial parameter estimation, along with Stereo-NEC's time-consuming keypoint tracking for gyroscope bias estimation, highlight the need for an enhanced approach. We propose a novel initialization method that improves translation accuracy by employing a 3 Degree-of-Freedom (DoF) Bundle Adjustment (BA) for the translation estimate while keeping the rotation estimate fixed. Unlike ORB-SLAM3's 6-DoF BA, our method independently updates the rotation estimate by incorporating IMU measurements and gyroscope bias, thus addressing the deficiencies of direct rotation estimation from stereo visual odometry in challenging scenarios. Extensive evaluations on the EuRoC dataset demonstrate the superior accuracy of our method compared to ORB-SLAM3. Notably, our method outperforms ORB-SLAM3 on the V2_03_difficult dataset, which is particularly challenging due to factors such as motion blur and illumination changes that complicate state estimation. These results highlight the robustness and reliability of our approach in diverse and demanding environments. Our method not only enhances initialization performance but also shows significant potential for practical applications in real-world visual-inertial state estimation tasks.environments.

REFERENCES

- [1] H. Song, C. Liu, and H. Dai, "Bundledslam: An accurate visual slam system using multiple cameras," in *2024 IEEE 7th Advanced Information Technology, Electronic and Automation Control Conference (IAEAC)*, vol. 7, 2024, pp. 106–111.
- [2] Y. Yang, B. P. Wisely Babu, C. Chen, G. Huang, and L. Ren, "Analytic combined imu integration (aci2) for visual inertial navigation," in *2020 IEEE International Conference on Robotics and Automation (ICRA)*, 2020, pp. 4680–4686.
- [3] Y. Yang, P. Geneva, and G. Huang, "Multi-visual-inertial system: Analysis, calibration and estimation," *The International Journal of Robotics Research*, 2024.
- [4] T. Qin, T. Chen, Y. Chen, and Q. Su, "Avp-slam: Semantic visual mapping and localization for autonomous vehicles in the parking lot," in *2020 IEEE/RSJ International Conference on Intelligent Robots and Systems (IROS)*, 2020, pp. 5939–5945.
- [5] L. Mescheder, M. Oechsle, M. Niemeyer, S. Nowozin, and A. Geiger, "Occupancy networks: Learning 3d reconstruction in function space," in *Proceedings of the IEEE/CVF conference on computer vision and pattern recognition*, 2019, pp. 4460–4470.
- [6] X. Zhang, J. Chen, Q. Wang, W. Xiong, X. Chen, and H. Yang, "Estimation of extrinsic parameters with trifocal tensor for intelligent vehicle-mounted cameras," *IEEE/ASME Transactions on Mechatronics*, vol. 27, no. 4, pp. 2107–2115, 2022.
- [7] X. Zhang, J. Chen, J. Deng, R. Wang, W. Xiong, and Q. Wang, "Structure and motion for intelligent vehicles using an uncalibrated two-camera system," *IEEE Transactions on Industrial Electronics*, vol. 70, no. 2, pp. 1772–1782, 2023.
- [8] J. Feng, L. Yang, E. Hoxha, B. Jiang, and J. Xiao, "Robotic inspection of underground utilities for construction survey using a ground penetrating radar," *Journal of Computing in Civil Engineering*, vol. 37, no. 1, p. 04022049, 2023.
- [9] E. Hoxha, J. Feng, D. Sanakov, and J. Xiao, "Robotic inspection and subsurface defect mapping using impact-echo and ground penetrating radar," *IEEE Robotics and Automation Letters*, 2023.
- [10] H. Li, M. Kutbi, X. Li, C. Cai, P. Mordohai, and G. Hua, "An egocentric computer vision based co-robot wheelchair," in *2016 IEEE/RSJ International Conference on Intelligent Robots and Systems (IROS)*, 2016, pp. 1829–1836.
- [11] Z. Chen, Z. Ding, D. J. Crandall, and L. Liu, "Polyline generative navigable space segmentation for autonomous visual navigation," *IEEE Robotics and Automation Letters*, vol. 8, no. 4, pp. 2054–2061, 2023.
- [12] T. Qin, P. Li, and S. Shen, "VINS-Mono: A robust and versatile monocular visual-inertial state estimator," *IEEE Transactions on Robotics*, vol. 34, no. 4, pp. 1004–1020, 2018.
- [13] R. Mur-Artal and J. D. Tardos, "ORB-SLAM2: An open-source SLAM system for monocular, stereo, and RGB-d cameras," *IEEE Transactions on Robotics*, vol. 33, no. 5, pp. 1255–1262, Oct. 2017.
- [14] W. Ye, X. Lan, S. Chen, Y. Ming, X. Yu, H. Bao, Z. Cui, and G. Zhang, "Pvo: Panoptic visual odometry," in *Proceedings of the IEEE/CVF Conference on Computer Vision and Pattern Recognition (CVPR)*, Jun. 2023, pp. 9579–9589.
- [15] L. Gao, G. Cordova, C. Danielson, and R. Fierro, "Autonomous multi-robot servicing for spacecraft operation extension," in *2023 IEEE/RSJ International Conference on Intelligent Robots and Systems (IROS)*, IEEE, 2023, pp. 10 729–10 735.
- [16] M. Xanthidis, B. Joshi, M. Roznere, W. Wang, N. Burgdorfer, A. Q. Li, P. Mordohai, S. Nelakuditi, and I. Rekleitis, "Towards mapping of underwater structures by a team of autonomous underwater vehicles," in *The International Symposium of Robotics Research*, Springer, 2022, pp. 170–185.
- [17] W. Shi, R. Zhu, and S. Li, "Pairwise adversarial training for unsupervised class-imbalanced domain adaptation," in *Proceedings of the 28th ACM SIGKDD conference on knowledge discovery and data mining*, 2022, pp. 1598–1606.
- [18] Z. Chen and L. Liu, "Navigable space construction from sparse noisy point clouds," *IEEE Robotics and Automation Letters*, vol. 6, no. 3, pp. 4720–4727, 2021.
- [19] M. Xanthidis, B. Joshi, N. Karapetyan, M. Roznere, W. Wang, J. Johnson, A. Quattrini Li, J. Casana, P. Mordohai, S. Nelakuditi, et al., "Towards multi-robot shipwreck mapping," in *Advanced Marine Robotics Technical Committee Workshop on Active Perception at IEEE International Conference on Robotics and Automation (ICRA)*, 2021.
- [20] W. Wang, B. Joshi, N. Burgdorfer, K. Batsosc, A. Q. Lid, P. Mordohai, and I. Rekleitis, "Real-time dense 3d mapping of underwater environments," in *2023 IEEE International Conference on Robotics and Automation (ICRA)*, 2023, pp. 5184–5191.
- [21] J. Feng, L. Yang, and J. Xiao, "Subsurface object 3d modeling based on ground penetration radar using deep neural network," *Journal of Computing in Civil Engineering*, vol. 37, no. 6, p. 04023030, 2023.
- [22] L. Chen, W. Wang, and P. Mordohai, "Learning the distribution of errors in stereo matching for joint disparity and uncertainty estimation," in *Proceedings of the IEEE/CVF Conference on Computer Vision and Pattern Recognition (CVPR)*, Jun. 2023, pp. 17 235–17 244.
- [23] C. Cai, P. Ji, Q. Yan, and Y. Xu, "Riav-mvs: Recurrent-indexing an asymmetric volume for multi-view stereo," in *Proceedings of the IEEE/CVF Conference on Computer Vision and Pattern Recognition (CVPR)*, Jun. 2023, pp. 919–928.
- [24] K. Batsos, C. Cai, and P. Mordohai, "Cbmvs: A coalesced bidirectional matching volume for disparity estimation," in *Proceedings of the IEEE Conference on Computer Vision and Pattern Recognition (CVPR)*, Jun. 2018.
- [25] X. Yang, H. Li, H. Zhai, Y. Ming, Y. Liu, and G. Zhang, "Vox-fusion: Dense tracking and mapping with voxel-based neural implicit representation," in *2022 IEEE International Symposium on Mixed and Augmented Reality (ISMAR)*, 2022, pp. 499–507.
- [26] Z. Chen, Q. Yan, H. Zhan, C. Cai, X. Xu, Y. Huang, W. Wang, Z. Feng, L. Liu, and Y. Xu, *Planarnerf: Online learning of planar primitives with neural radiance fields*, 2023.
- [27] J. Liu, P. Ji, N. Bansal, C. Cai, Q. Yan, X. Huang, and Y. Xu, "Planemvs: 3d plane reconstruction from multi-view stereo," in *Proceedings of the IEEE/CVF Conference on Computer Vision and Pattern Recognition (CVPR)*, Jun. 2022, pp. 8665–8675.
- [28] L. Kneip, A. Martinelli, S. Weiss, D. Scaramuzza, and R. Siegwart, "Closed-form solution for absolute scale velocity determination combining inertial measurements and a single feature correspondence," in *IEEE International Conference on Robotics and Automation (ICRA)*, 2011, pp. 4546–4553.
- [29] A. Martinelli, "Closed-form solution of visual-inertial structure from motion," *International Journal of Computer Vision (IJCV)*, vol. 106, no. 2, pp. 138–152, 2014.
- [30] J. Kaiser, A. Martinelli, F. Fontana, and D. Scaramuzza, "Simultaneous state initialization and gyroscope bias calibration in visual inertial aided navigation," *IEEE Robotics and Automation Letters*, vol. 2, no. 1, pp. 18–25, 2017.
- [31] T. Dong-Si and A. I. Mourikis, "Estimator initialization in vision-aided inertial navigation with unknown camera-IMU calibration," in *IEEE/RSJ International Conference on Intelligent Robots and Systems (IROS)*, 2012, pp. 1064–1071.
- [32] C. Campos, J. M. M. Montiel, and J. D. Tardós, "Fast and robust initialization for visual-inertial slam," in *IEEE International Conference on Robotics and Automation (ICRA)*, 2019, pp. 1288–1294.
- [33] R. Mur-Artal and J. D. Tardós, "Visual-Inertial monocular SLAM with map reuse," *IEEE Robotics and Automation Letters*, vol. 2, no. 2, pp. 796–803, 2017.
- [34] W. Huang and H. Liu, "Online initialization and automatic camera-imu extrinsic calibration for monocular visual-inertial slam," in *IEEE International Conference on Robotics and Automation (ICRA)*, 2018, pp. 5182–5189.
- [35] C. Campos, J. M. M. Montiel, and J. D. Tardós, "Inertial-only optimization for visual-inertial initialization," in *IEEE International Conference on Robotics and Automation (ICRA)*, 2020, pp. 51–57.
- [36] W. Wang, J. Li, Y. Ming, and P. Mordohai, "EDI: ESKF-based Disjoint Initialization for Visual-Inertial SLAM Systems," in *Proceedings of IEEE/RSJ International Conference on Intelligent Robots and Systems (IROS)*, 2023.
- [37] P. Geneva, K. Eickenhoff, W. Lee, Y. Yang, and G. Huang, "Open-VINS: A research platform for visual-inertial estimation," in *IEEE International Conference on Robotics and Automation (ICRA)*, 2020, pp. 4666–4672.
- [38] W. Huang, H. Liu, and W. Wan, "An online initialization and self-calibration method for stereo visual-inertial odometry," *IEEE Transactions on Robotics*, vol. 36, no. 4, pp. 1153–1170, 2020.
- [39] P. Chen, W. Guan, and P. Lu, "ESVIO: Event-based stereo visual inertial odometry," *IEEE Robotics and Automation Letters*, vol. 8, no. 6, pp. 3661–3668, 2023.

- [40] T. Qin, S. Cao, J. Pan, and S. Shen, "A general optimization-based framework for global pose estimation with multiple sensors," *arXiv preprint arXiv:1901.03642*, 2019.
- [41] C. Campos, R. Elvira, J. J. Gómez, J. M. M. Montiel, and J. D. Tardós, "ORB-SLAM3: An accurate open-source library for visual, visual-inertial and multi-map SLAM," *IEEE Transactions on Robotics*, vol. 37, no. 6, pp. 1874–1890, 2021.
- [42] W. Wang, C. Chou, G. Sevagamoorthy, K. Chen, Z. Chen, Z. Feng, Y. Xia, F. Cai, Y. Xu, and P. Mordohai, "Stereo-nec: Enhancing stereo visual-inertial slam initialization with normal epipolar constraints," *arXiv preprint arXiv:2403.07225*, 2024.